

HOSTED BY



ELSEVIER

Contents lists available at ScienceDirect

# Engineering Science and Technology, an International Journal

journal homepage: [www.elsevier.com/locate/jestech](http://www.elsevier.com/locate/jestech)

Full Length Article

## Engineering design of plasma generation devices using Elmer finite element simulation methods

Daniel Bondarenko<sup>a</sup>, Hossam A. Gabbar<sup>a,b,\*</sup>, C.A. Barry Stoute<sup>b</sup><sup>a</sup> Faculty of Engineering and Applied Science, University of Ontario Institute of Technology, 2000 Simcoe Street North, Oshawa L1H7K4, ON, Canada<sup>b</sup> Faculty of Energy Systems and Nuclear Science, University of Ontario Institute of Technology, 2000 Simcoe Street North, Oshawa L1H7K4, ON, Canada

## ARTICLE INFO

## Article history:

Received 7 March 2016

Revised 26 July 2016

Accepted 26 July 2016

Available online xxx

## Keywords:

Elmer simulation  
Plasma generation  
FEM simulation

## ABSTRACT

Plasma generation devices are important technology for many engineering disciplines. The process for acquiring experience for designing plasma devices requires practice, time, and the right tools. The practice and time depend on the individual and the access to the right tools can be a limiting factor to achieve experience and to get an idea on the possible risks. The use of Elmer finite element method (FEM) software for verifying plasma engineering design is presented as an accessible tool that can help modeling multi-physics and verifying plasma generation devices. Furthermore, Elmer FEM will be suitable for experienced engineer and can be used for determining the risks in a design or a process that use plasma. A physical experiment was conducted to demonstrate new features of plasma generation technology where results are compared with plasma simulation using Elmer FEM.

© 2016 Karabuk University. Publishing services by Elsevier B.V. This is an open access article under the CC BY-NC-ND license (<http://creativecommons.org/licenses/by-nc-nd/4.0/>).

### 1. Introduction and background

The design of plasma employing devices is a complex process demanding experience and skill that can be acquired with practice and time. The access to the laboratory equipment for prototyping of plasma devices can be expensive and hazardous to health, especially when the preliminary models are not sufficiently understood. It is possible to gain a perspective on the basic plasma physics by investigating the process specific parameters, although, it would be best to visualize any these behaviors in the process. Therefore, a multi-physics tool suitable for modeling plasma behavior would be beneficial to have a handle on the process parameters and variables. The training of engineers to familiarize with plasma processes is critical for achieving reasonable outputs from the plasma simulations, as would be the case for the engineers dealing with structural analysis, heat transfer, or computational fluid dynamics (CFD). Respectively, certain simulation tools are available commercially and the licensing for their use is available, other simulation tools are available as a result of the government research and made available to the public and academia under that government. The use of the government provided soft-

ware is unlike the commercial software due to the level of detail and certain aspects of user interface. Elmer FEM is a hybrid case of a multi-physics software that was developed for the national CFD program by a chain of Finnish universities and in collaboration with engineering industries in 1997, and it was licensed under GNU public license in 2005 [1]. This software has a significant foundation that can be used in training of the aspiring plasma physicists and engineers if the case studies of plasma behaviors can be validated. Hence, the objective of finding and validating possible case studies was found worthwhile pursuing because it would allow for a wider range of interested engineers to gain experience in modeling plasma phenomena and allow to estimate the regions of risk and danger in the devices using plasma processes. Education and the access to the right tools can help in making designs that are safe and testing such tools is an essential step to validating their applicability [2,3].

The theory describing the flows interacting with the electromagnetic fields has been actively used for modeling liquid metals. The complex fluid behavior of plasma is unlike the metal flows due to its compressible properties and unique qualities of Coulomb interactions [4]. The foundational plasma research involved the plasma flow interactions with the electromagnetic fields, which lead to the culmination of fluid dynamics and electro-dynamic theories, generally confined to the study of Magneto-Hydro-Dynamics (MHD) [4].

The FEM discretization is based on a piecewise representation of the solution in terms of the basic functions [5]. The computational

\* Corresponding author at: Faculty of Energy Systems and Nuclear Science, and Faculty of Engineering and Applied Science, University of Ontario Institute of Technology, 2000 Simcoe Street North, Oshawa L1H7K4, ON, Canada.

E-mail address: [Hossam.gabbar@uoit.ca](mailto:Hossam.gabbar@uoit.ca) (H. A. Gabbar).

Peer review under responsibility of Karabuk University.

<http://dx.doi.org/10.1016/j.jestech.2016.07.015>

2215-0986/© 2016 Karabuk University. Publishing services by Elsevier B.V.

This is an open access article under the CC BY-NC-ND license (<http://creativecommons.org/licenses/by-nc-nd/4.0/>).

### Nomenclature

Symbol	Definition		
<b>B</b>	magnetic field (T)	$p$	pressure (Pa)
<b>E</b>	electric field (V/m)	$q_e$	electron charge ( $1.602 \cdot 10^{-19}$ C)
$E$	Energy (J)	$t$	time
$h$	Planck constant ( $6.626 \cdot 10^{-34}$ J s)	$T$	temperature (K)
$I$	current (A)	$T_e$	electron temperature (K or eV)
$J$	current density (A/m <sup>2</sup> )	$\mathbf{v}$	velocity of particle or fluid (m/s)
$k_B$	Boltzmann constant ( $1.380 \cdot 10^{-23}$ J/K)	$V$	voltage (V)
$m$	total mass (kg)	$\eta_{\text{opt-Air}}$	Stoletov constant (81 eV/ion-electron pair)
$\dot{m}$	mass flow rate (kg/s)	$\Theta$	heat flux (W/m <sup>2</sup> )
$M$	molecular mass (kg/kmol)	$\mu$	viscosity (Pa·s)
$n$	number of particles (electrons, ions per m <sup>3</sup> )	$\sigma_p$	plasma conductivity (S/m)
		$\rho$	density (kg/m <sup>3</sup> )

domain of the body of interest is divided up into smaller, finite element, domains and the solution in each element is constructed from the basic functions. The equations solved are typically obtained by restating the conservation equation in a weak form: the field variables are written in terms of the basic functions, the equation is multiplied by appropriate test functions, and then integrated over an element [5]. For Elmer FEM a system of multi-physics equations that encompass MHD phenomena can be obtained for plasma, and solved based on the initial and boundary conditions set into the simulation. The design safety can be

achieved for the plasma devices by following through with a design approach outlined in the following flow chart, as shown in Fig. 1 [6].

The flow chart provides a process for the design approach with intrinsic focus on safety, where the design features are considered to be approached with an engineering design grounded in physical and safety foundations. This approach makes sense when the key tool for the design validation is tested. In present work, the first column of the chart is used in the method of approach, and the second and third column are used in the section on results and discussions respectively.

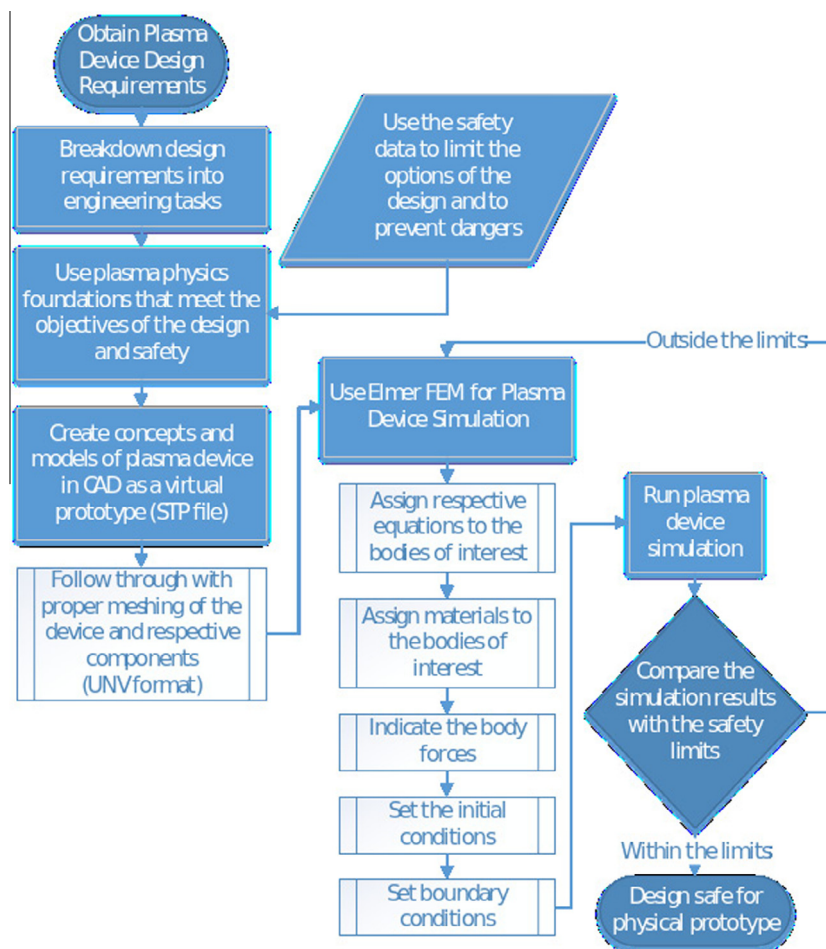


Fig. 1. Plasma device design flow-chart process using Elmer FEM [1].

The proposed research will support number of industries such manufacturing, one example is shown in cutting applications [16].

## 2. Method of approach

The method for validating the performance of plasma simulation by Elmer FEM is conducted by an experiment. First, a physical prototype of a direct discharge plasma generator is made with the data acquisition instrumentation. A model of the generator is reproduced in Elmer FEM and the results of the simulation are compared to the results of the experiment.

In the experiment, it is assumed that the plasma working gas is air that is dry and has a molar mass is roughly 28.9645 g/mol at standard ambient temperature and pressure (SATP). It is also assumed that the plasma behaves closely to an ideal gas, since the conditions are near vacuum and the collisional effects are far below the levels of fusion scenarios. The continuity of fluid behavior in the experiment is assumed to remain valid. Lastly, the pressures of plasma are expected not to exceed the SATP conditions, hence the convection of fluids is possible [7,8].

Fig. 2 presents a schematic of the plasma generator experiment and Fig. 3 presents the physical layout. The most notable experiment risks in this configuration include the use of high voltage and high current electrical equipment under vacuum conditions.

The corresponding risk components needed to be handled in the experiment include a 9000 V transformer and 3.8 L vacuum chamber. The radio-frequency (RF) circuit combined with the DC power supply is intended for future work when a stable source is obtained for investigating plasma resonance phenomena, as of current time the results of RF assisted configuration are pending review. Fig. 4 presents the plasma generating end of the experiment. This nozzle and probe configuration has to be pre-assembled onto the vacuum chamber lid prior to the conduction of any experiments. Respectively, there is a safety procedure for working with this configuration. A person responsible for assembling this working end is required to use the utmost care during handling. The use of insulating surgery gloves are highly advised to prevent the contamination of the components by any alien contaminants. In case the device is deemed to have been contaminated, it is advised to use cotton damped with a 99% propanol solution and clean any of the surfaces under suspicion. Lastly, the plasma generator assembly with lid of the vacuum chamber needs to evaporate any of the propanol remnants before being mounted onto the steel vacuum chamber.

The primary control mechanisms of the plasma generation process in the experiment include the activation of the high voltage transformer and the control of the gas inflow via the insulated inlet valve. Provided the relatively crude assembly of the experiment,

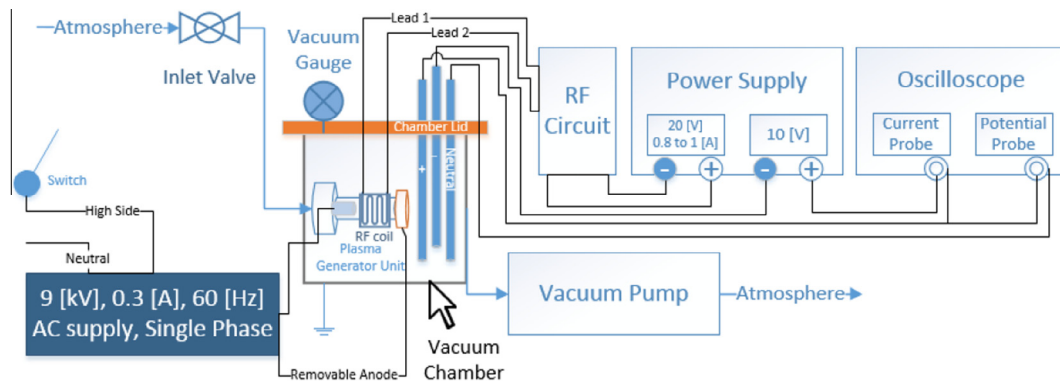


Fig. 2. Schematic layout for direct discharge plasma experiment.

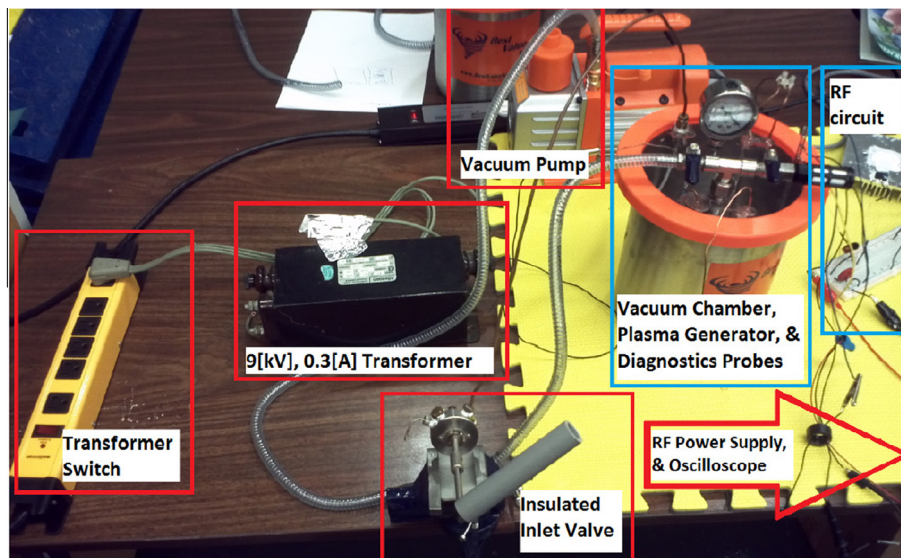


Fig. 3. Physical layout for the direct arc discharge experiment.



the awareness of these control components and their careful utilization are essential to keeping the investigators and the experiment safe.

The process measurement and data acquisition allows to evaluate the critical plasma variables. In the experiment presented, there are four primary variables that can assist in determining the properties of plasma: vacuum pressure, power used in generator, and the combination of current and potential readings from the triple Langmuir probe.

The pressure inside the vacuum chamber is measured using the pressure gauge, and as far the practical experiments allow, this measurement proved to be quite sufficient to indicate the gas flow rate into the plasma generator; the velocity of the flow entering into the plasma generator was measured to be 9.701 m/s. The power use of the plasma generator is found by taking the readings of the potential and current supplied by the device as set by the power supply, in the case of the transformer it is rated to provide alternating current at 9000 V and 30 mA, or a power of 270 W. The voltage and current of a plasma often fluctuate, hence, the RMS values are used [9]. If the measurements are taken at the generator side, in term of the power used from the power grid, it is possible to use digital means. However, if the readings are taken directly at the plasma, the conventional digital meters may not be reliable due to the high-frequency behavior of the plasma. Hence the measurement of power used by the device is measured from the grid side, and compared to the power used by the coupling coil. If the voltage and current are stable, the analog or digital instruments calibrated for DC, average, or RMS waveforms can be used [9].

The triple Langmuir probe is slightly more detailed and involved in terms of the plasma diagnostics, as it helps to determine the electron temperature,  $T_e$ , the current density,  $J_{plas}$ , and the electron density,  $n_e$ . The circuit detail of the triple Langmuir probe (TLP) is presented in Fig. 5, where the three rods are conductive tungsten probes exposed to plasma.

There are two variables that are measured directly using this probe: the potential across a positive lead and a neutral lead (V in the Fig. 5), and the current conducted by the plasma between the positive and the negative leads (A in the Fig. 5). The potential supplied by a steady potential source is set to 10 V and it has shown to be sufficiently reliable to yield a maximum systematic error of 15% in similar experiments [10,11]. In order to find the electron temperature, the current density, and the electron density, the formulas derived via an experiment are [11]

$$T_e = \frac{V}{\ln(2)} \text{ [eV]} \tag{1a}$$

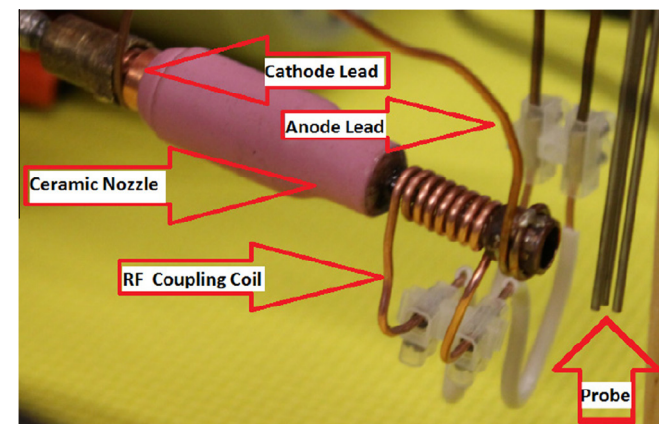


Fig. 4. Plasma generator assembly.

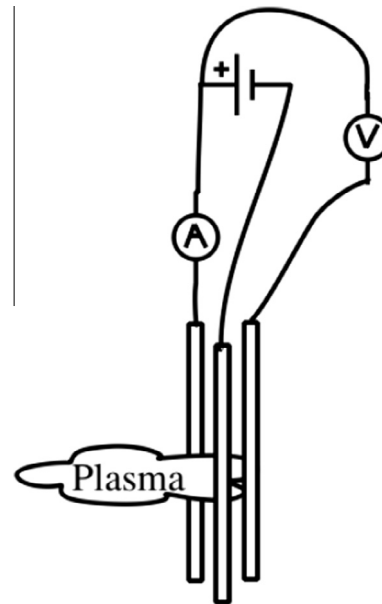


Fig. 5. Circuit diagram of the triple Langmuir probe.

$$J_{plas} = \frac{\frac{A}{ProbeArea} * 1}{10^{\frac{V}{T_e}} - 1} \text{ [A/m}^2\text{]} \tag{1b}$$

$$n_e = \frac{J_{plas} \cdot \exp(\frac{1}{2})}{q_e \sqrt{q_e \cdot \frac{T_e}{m_i}}} \text{ [particles]} \tag{1c}$$

The probe area is the area of plasma contact with the probe, in the experiment it was found to be 0.0002005 m<sup>2</sup>, by using the Vernier caliper and measuring an area of probe's thermal discoloration at the end of experiments. The voltage and current may vary from cycle to cycle in the plasma generating processes where plasma can move and be affected by the supply gas flow. When the plasma voltage and current fluctuate with time the only true measurement of these quantities can be made using an oscilloscope [9]. Hence, there are some errors encountered in the TLP. When the probe is inserted into plasma, its electrically conducting surface superimposes an equi-potential in the plasma region thereby forming a space charge and flow of current between the probe leads [8]. A space charge preserves charge equilibrium in the plasma. The electrons have a much higher velocity than the ions and they strike the probe more and form a negative space charge due to the few slow-moving positive ions in the region [11]. The problem of disrupting the plasma is overcome partially by the Langmuir probe via application of a bias voltage to the probe and nullifying the current flow from the plasma, so that a floating potential V is produced equal to the local potential in the undisturbed plasma [11]. Also, by making the probe diameter very much less than the principal dimensions of the plasma and the probe face, leads to minimization of the effect on the local electric field in the plasma. In the experiment the chamber pressure is maintained at 7.2 kPa, and the use of the TLP provides fair results that can be used for verifying computational simulations [11]. Also, the multitude of samples for the potential and the current attained from the TLP are normalized to have average values with a specific standard deviation based on the samples.

The method of plasma generator simulation is entwined with multi-physical descriptions of sub-systems and components. These descriptions are distinguished for each composing part of the overall plasma generator and combined in order to produce a model matching with the experiment. The dimensions for the experiment

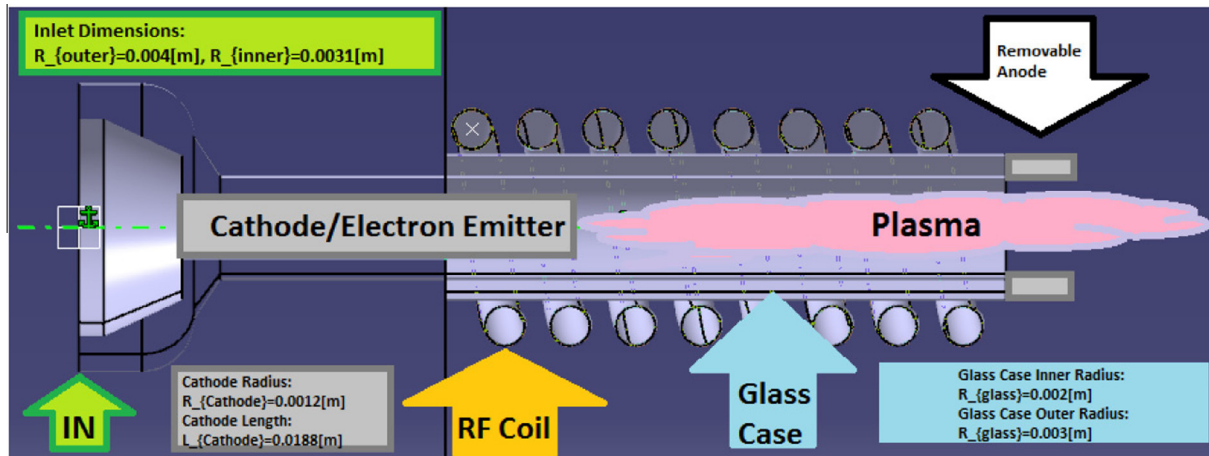


Fig. 6. Plasma generator working region model.

and the key components of the plasma generator are highlighted in Fig. 6.

The conditions for the plasma simulation are as follows:

1. The mesh size near the boundary walls is set to 0.05 mm.
2. The peak velocity of the gas entering the plasma generation region is 9.701 m/s.
3. The Large Eddy Simulation is conducted under the assumption of plasma viscosity equivalent to  $1.983 \cdot 10^{-5}$  kg/(m·s) and at a Smagorinsky constant of 0.1.
4. The plasma heat conductivity is approximated to be nearly equivalent to the air conductivity 0.002 W/(m·K).
5. The reference Temperature is 297.15 K and the reference pressure is 7.181 Pa.
6. The electric conductivity near the electrodes is  $1.689 \cdot 10^{-5}$  S/m.
7. The heat capacity of the air plasma has been approximated to be 1005 J/K with the air density being 0.084 [kg/m<sup>3</sup>].

In order to model the plasma gas supply source, it is necessary to consider the compressibility of gases entering the plasma chamber, the boundary layers that would occur near the chamber walls, and the ionization energies of the gases, and the behavior under turbulent conditions. The gas supply has to provide a controlled amount of substance to sustain plasma without extinguishing it, and, at the same time, it has to keep the generator chamber walls cool. The use of Elmer is suitable for complex multi-physics models, although it will also be crucial to consider the effects of heat transfer and possible back-flows that pose a danger of affecting the plasma generator structurally as well as impeding the flow and de-stabilizing the plasma generation regime. The modeling of the plasma exiting the generation and confinement region will be based on fluid behavior and the effectiveness of the acting nozzle. The plasma initiation region is created via the high-field electron emission. The process of ionization occurs due to the stripping of electrons from the atoms of working gas, thereby creating a focused region of charged particles. This region can be shifted depending on the requirements for plasma generation and confinement. The modeling methodology of the ionizing configuration is intrinsically complex and deals with matters bordering quantum mechanics. However, it is possible to model the interaction with working gases and plasma by the use of the FEM. The plasma generator device will primarily depend on the combined performance of the high-field emitter the arc coupling, flow of the working gas, and heat transfer effects. The collisional effects and the particle retention will be of the main interest in terms of the similarity to the experiment, hence the temperature of the flow, the plasma

current and the behavior of the ionized species attained by the simulation will be compared to the experimental results. The associated toolboxes that have been used in the plasma simulation process are presented in Fig. 7, below [1].

### 3. Fundamental theory and calculations for Elmer FEM

The importance of familiarizing engineers with the plasma phenomena and its risks is not only in the matter of plasma being a hot ionized gas that can violently react depending on the surrounding chemicals, it is also able to interfere with sensitive electronics and lead to irreparable damage. For modeling of plasma devices, the use of Elmer FEM requires some fundamental understanding of plasma physics, MHD, and the property interactions of between the plasma and the boundaries. The full set of a steady state MHD flow equations are the following:

$$\frac{\partial \rho}{\partial t} + \mathbf{v} \cdot \nabla \rho = 0, \quad (2a)$$

$$\frac{\partial \rho \mathbf{v}}{\partial t} + \mathbf{v} \cdot \nabla \rho \mathbf{v} = -\nabla p + \mu \nabla^2 \mathbf{v} - \nabla \left( \frac{2}{3} \mu \nabla \cdot \mathbf{v} \right) + \rho_q (\mathbf{E} + \mathbf{v} \times \mathbf{B}), \quad (2b)$$

$$\frac{\partial \mathbf{E}}{\partial t} + \mathbf{v} \cdot \nabla \mathbf{E} = \nabla \cdot \Theta + \left( \mu \nabla \cdot \mathbf{v} - \left( \frac{2}{3} \mu \nabla \cdot \mathbf{v} \right) \right) \cdot \mathbf{v} + \rho_q \mathbf{E} \cdot \mathbf{v}, \quad (2c)$$

$$\nabla \times \mathbf{E} = -\frac{\partial \mathbf{B}}{\partial t}. \quad (2d)$$

Equation set (2) is the equations of flow continuity, flow momentum, energy, and Faraday's law, respectively. The nomenclature of the equations is mentioned at the beginning of

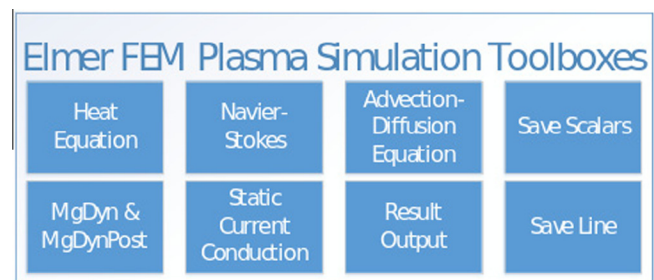


Fig. 7. Toolboxes used for plasma generator device in Elmer FEM.

the paper. The explanation of the equations is to be understood by the reader [4].

The reductive form of the turbulent flow under the simplified conditions does not make it easy to compute it along with the equations for the plasma behavior. Hence, although the methodology taken in modeling the plasma behavior implements the theoretical foundations presented, solving the Navier–Stokes equations with the MHD coupling terms even for the steady state flows would become an intensive mathematical challenge of solving complex partial differential equations. In order to avoid this cumbersome path the application of FEM for computing the fluid-dynamic changes at very fine meshes will be implemented through Elmer FEM as it can closely produce a solution via the use of a Large Eddy Simulation (LES) technique, which has the capacity to compete with the direct numerical simulation (DNS), provided it is done correctly [7,8].

The LES technique makes approximations, unlike the DNS method, though these approximations are based on the rigorous data sampling of actual flows. By and large, the LES method takes into account the physical phenomena and implements the ODEs with approximations based off the measurement of eddies in the experiment, thereby making the equation value models work together with the real-world data. The coupling to electric and magnetic fields can be expressed through a variable for external force acting on the fluid [7]. In electro-kinetics the fluid may have charges that are coupled to external electric fields and lead to an external force. The charge density may be a variable, depending on how quick the ions are generated and removed, although in steady state it can be approximated to be constant. Also, if the fluid has ionized species it will also couple with the magnetic field [12]. The diffusion–advection–convection effect in flow is the transport of scalar quantity of ionized species by diffusion, advection, and convection. The difference in the nomenclature usually indicates that an advected quantity does not have an effect on the velocity field of the total fluid flow, and a convected quantity as in [1]. The diffusion–advection–convection effect is derived from the principle of mass conservation of each species in the fluid mixture and may have sources or sinks either at the boundary conditions or within the body of plasma. Hence, multiple advection–diffusion equations may be coupled together to analyze plasma interaction in mixtures and convective flows at different temperatures. If the velocity field is zero, then the advection–diffusion equation reduces to the diffusion equation, which is applicable only in solids [7].

The modeling of the direct discharge plasma generation uses the multi-physics Elmer FEM toolboxes based on the estimations of the plasma properties. The key property to modeling the plasma discharge is the plasma conductivity. Provided all the initial and boundary conditions were set correctly the limits of the electron temperature, the current density, and the electron density will be determined by this property. For the sake of modeling with available computing power, it was assumed that the plasma is quasi-neutral, and that the resistive modeling of plasma is applicable. The conductivity computation for the plasma can be roughly estimated as a ratio of current passing between the surfaces at ionizing potential. The simulation critical variables known prior to the configuration of the experiment and the simulation include the current in the arc discharge ( $I = 0.152$  A), the potential ( $V = 9000$  V), the reference pressure ( $P_{\text{ref}} = 7180.8$  Pa = 53.86 Torr), and the RMS mass transfer coefficient between the electrons and ions  $\frac{m_e}{m_i} \cdot \frac{1}{\sqrt{2}} = 1.36 \cdot 10^{-5}$  [13]. Based on the current and the potential it is possible to attain an approximate ion–electron generation rate, using the Stoletov constants ( $\eta_{\text{opt-Air}} = 81$  eV/ion–electron pair) and the following relation, where,  $q_e$  is the fundamental charge unit  $1.602 \cdot 10^{-19}$  C [14]:

$$n_e = \frac{I \cdot V}{\eta_{\text{opt-Air}} \cdot q} \quad (3)$$

In Elmer FEM, the concentration at the boundary is expressed as a ratio to the number of available neutral particles. In the current case, the rate of neutral particles entering the chamber corresponds to the flow rate found to be  $2.47 \cdot 10^{20}$  particles/s. The ratio of these rates yields a value that is interpreted by Elmer for computing the ion behaviors in the plasma 0.426415 ion/particles. The concentration flux is the other parameter necessary to compute the plasma behavior, it is approximated at the emitter to roughly correspond the number of ions passing through the area confined by the glass (ceramic) chamber  $\text{Flux}_{\text{Area}} = 1.257 \cdot 10^{-5}$  m<sup>2</sup>. The equation for concentration flux states:

$$\frac{\dot{M}_i}{\text{Flux}_{\text{Area}}} = \frac{\dot{n}_i \cdot m_i}{\text{Flux}_{\text{Area}}} \quad (4)$$

For the direct discharge mode, the concentration flux is computed to be 0.397 kg/m<sup>2</sup> as required to set the boundary conditions in Elmer FEM. If plasma is unaffected by the flow the theoretical plasma temperature can be estimated using the Saha equation [15] to yield 23365 K or 2.014 eV. This value showcases an upper limit to the ideal quasi-neutral plasma state provided that the species have indeed ionized fully and neither any external flow nor any heat dissipative sinks are present. The computation of the expected current density reading range and the expected Joule heating parameter are based on the Elmer FEM models manual [1]. Although, the plasma conductivity can be obtained from the experiment for the direct discharge configuration, the attainment of this parameter for the single emitter condition is made significantly easier by approximating the conductivity based on the potential available at the emitters and the emission current.

#### 4. Results and discussions

It is worthwhile to consider the implications of experimental data with respect to the limitations of the triple Langmuir probe. As mentioned before, the maximum error in the case of the triple Langmuir probe can reach 15% of the measured value. The experimental data samples for the current and the potential readings from the TPL are presented in the Figs. 8 and 9, respectively. The samples have been normalized to a bell curve with 36 samples for the current readings and 52 samples for the potential readings.

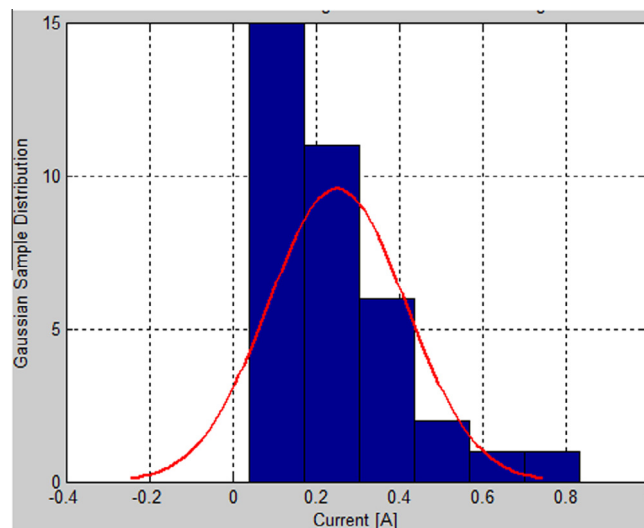


Fig. 8. Bell curve for the TLP current readings.



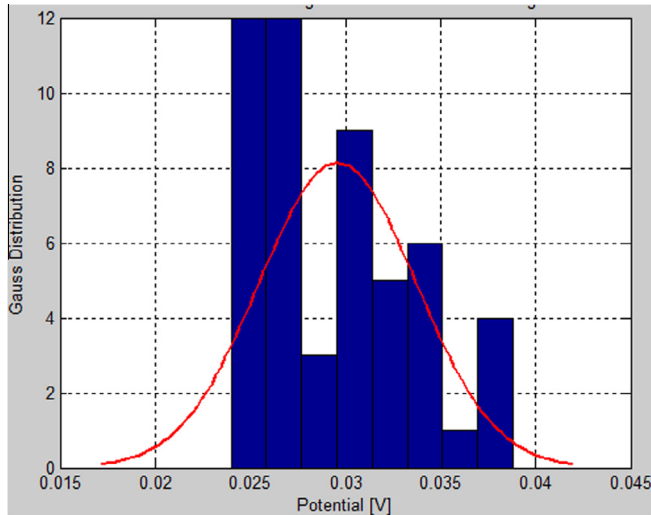


Fig. 9. Bell curve for the TLP potential readings.

Table 1

The plasma properties for the direct discharge configuration measured using TLP.

Method	$T_e$ [eV]	$J_{\text{plas}}$ [A/m <sup>2</sup> ]	$n_e$ [m <sup>-3</sup> ]
Direct discharge min.	0.036	1800	$0.93 \cdot 10^{20}$
Direct discharge ave.	0.043	2100	$1.09 \cdot 10^{20}$
Direct discharge max.	0.049	2400	$1.26 \cdot 10^{20}$
Simulation results	0.043	12,000	$1.30 \cdot 10^{20}$

Based on the averaged experimental findings, the electron temperature (Eq. (1a)), the current density (Eq. (1b)), and the electron density (Eq. (1c)) have been computed. The average values in terms of the maximums and minimums, in accordance with the 15% error of the TLP, as well as the results obtained from Elmer FEM, are indicated in Table 1.

Provided that the measurement using the triple Langmuir probe do not yield the exact values, it is useful nonetheless to have a range of values at minimal and maximal errors. Using a hypothesis testing approach for the Gaussian distribution in terms of the electron Temperature and density, it is possible to have a 99.9% confidence that the results obtained by the simulation are in accordance with experimental observations. Furthermore, although the equipment setting that was used for the experimentation is not on par with a high budget lab, it does the job it was set out to do. As far as the experimental results are concerned (as made evident in the table above), the experimental setting has done a good job in verifying the functionality of Elmer FEM as a tool for modeling plasma phenomena. The figures below are representative of the results for the direct discharge and include the properties of plasma such as temperature, the ion-to-neutrals concentration ratio, current, and the magnetic strength.

Figs. 10–13 showcase the results obtained from the Elmer FEM solver for the direct plasma discharge at the conditions equivalent to those observed in the experiment. Fig. 10 showcases the temperature distribution of the plasma with the regions of highest temperature located near the electrodes.

The Fig. 11 presents the ion concentration ratio for the region of plasma generation with respect to the gas particles available in the chamber. The highest concentration of the ionized particles is shifted to the left of the cathode due to the flow carrying the ionized particles from their source of origin. On other hand, Fig. 12 shows the current per unit length (A/m) profile for the arc discharge and showcases that despite the high electron concentration not all the electrons are able to contribute to the ionization process

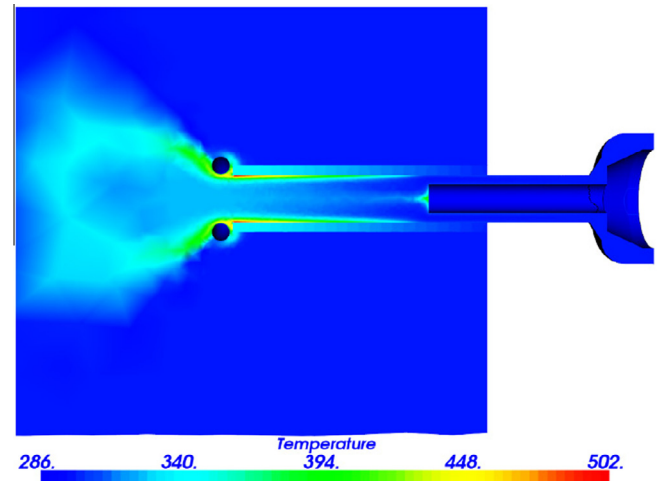


Fig. 10. Plasma temperature profile in Kelvins.

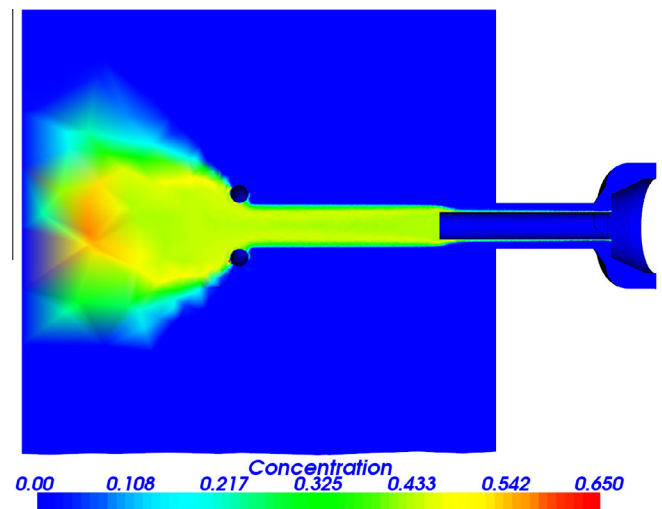


Fig. 11. Ion concentration ratio profile from 0% to 65%.

observed in Fig. 11 due to their low energy and the passing through the gas without collision with the neutral gas. The electric current in the gas results in the magnetic field distribution near the electrodes that is showcased in Fig. 13. The magnetic field is focused near the rightmost electrode dominates in the cross section profile due to the emission near the sharp tip.

Based on the experimental findings and the computational models it is possible to draw some conclusions to the matters of using Elmer FEM for simulations of the plasma generator. It is possible to implement the computer models and produce working concepts that are able to closely match the results of an experiment. However, several pitfalls of using equations prior to setting of an experimental model need to be addressed as it may become evident that there are discrepancies between what has been computed, and what has been found via an experiment and simulations, particularly made evident by the high current density in the simulation as compared to the experiment.

The reasons for the possible deviations between the experimental and simulation results include:

1. Secondary emission as a result of AC discharge; more electrons are generated as a result of alternating electric fields.
2. Spread of the electron flow onto the Langmuir probe; the electrons disperse and create a differentiating flow of ions.

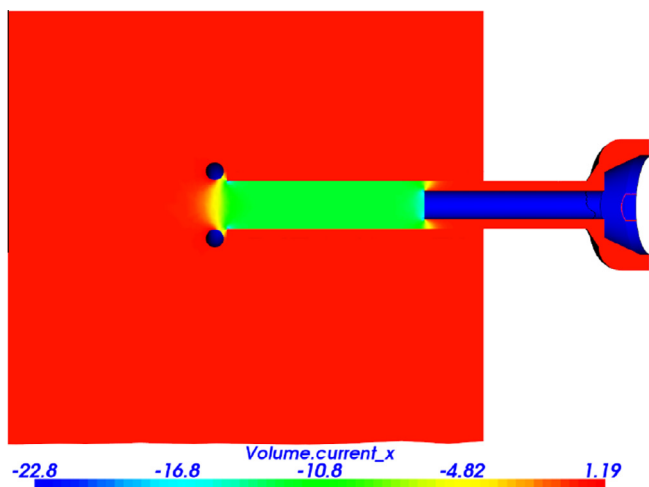


Fig. 12. Current per unit length of arc profile in A/m.

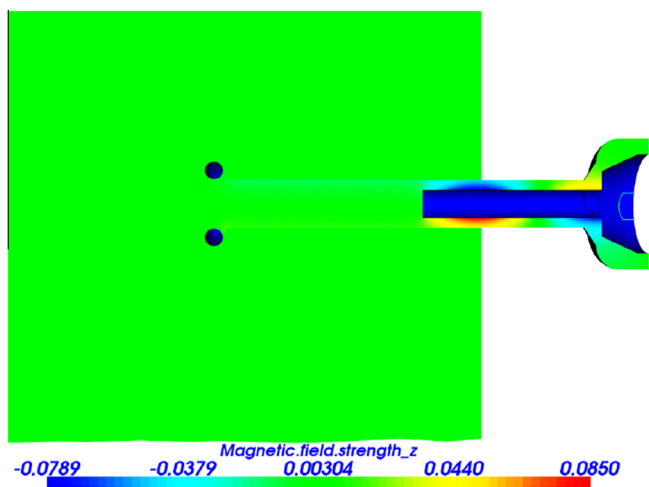


Fig. 13. Magnetic strength profile in mT.

3. Splattering effect from the walls; the electrons bombarding the back wall reflect back at the Langmuir probe due to the proximity of the wall and the secondary emission effects.
4. General flow effects; flow simply reflects back at the Langmuir probe due to the proximity of the wall.

It is worth noting that the differences between the results obtained by experiment and from the simulation are fairly small. The area of interest is near the outlet of the generator and in all cases it is relatively uniform. Nonetheless, the current density computed using the Elmer FEM far exceeds that of the current density obtained from the experiment. The reason for this deviation is in the fact that the Langmuir probe was picking up the current in the zone carried by the flow and outside the actual arc discharge. Also, the current in Elmer FEM is representative of the electron flow; so even though the values for the temperature and the ion concentrations were in the range reasonable with the experiment, the current densities do not match because Elmer FEM indicated the electron flow, unlike the ion flow detected by the TLP. By keeping in mind this distinction between the experiment and the simulation it is understandable that Elmer FEM can be used to model the plasma phenomena well enough to be closely matching to the physical reality.

## 5. Conclusions and future work

A functioning experiment was built to gather data for an arc discharge plasma generation device and to validate the performance of Elmer FEM as a tool for plasma modeling and skill acquisition tool. The simulation yielded the results that matched well with the experiment and therefore provide an indication that for the particular scenarios involving plasma discharges Elmer FEM is capable of providing sufficient results. Based on this study it is then possible for the interested engineers and practitioners to have physical backing to engage in the engineering design of plasma devices using Elmer FEM without subjecting themselves and their respective parties to the possible risks of exposure to the plasma.

For the academic work it would be interesting to implement a larger scale experiment and compare it with the performance of the standard plasma cutters that operate by the use of arc discharge. It would be also interesting to see the performance of the plasma generator device with a microwave passageway implemented and to analyze the regions of highest plasma activity in such a configuration. Furthermore, it is possible to utilize the Monte-Carlo algorithm in Elmer, although, in order to attain this feature in Elmer it is necessary to customize a code to be able to handle the interaction of ionized particles using dynamic statistics. The Direct Monte-Carlo algorithm may be implemented at the high-energy locations of plasmas interaction points and for instability tracking. Fortunately, Elmer FEM has the capacity to be altered and modified at the source code as well as have the ability to enact the custom made modeling toolboxes, and should be looked into further to increase the practical range of Elmer application in the engineering design of plasma devices. By following through with Elmer and by validating other modes of plasma in this program it would be possible also use it in design of plasma microwave tubes, fusion energy devices, particle accelerators, and design of plasma diagnostic devices. The industrial applications that can be derived from such research would then benefit the fields of medicine (cleaning and sanitization), communications (via the microwave technologies), lighting and laser devices, entertainment, and space propulsion.

## References

- [1] P. Raback, M. Malinen, J. Ruokolainen, A. Pursula, T. Zwinger, *Elmer Models Manual*, CSC IT Center for Science, Espoo, Finland, 2015.
- [2] C.C. Battaile, D.J. Srolovitz, Kinetic Monte Carlo simulation of chemical vapor deposition, *Annu. Rev. Mater. Res.* 32 (2002) 297–319.
- [3] P.A. Davidson, *An Introduction to Magnetohydrodynamics*, Cambridge University Press, Cambridge, 2001.
- [4] J. Howard, *Introduction to Plasma Physics*, Australian National University, Canberra, 2002.
- [5] J.F. Wendt, *Computational Fluid Dynamics*, Springer, Berlin Heidelberg, 2009.
- [6] C.-D. Munz, M. Auweter-Kurtz, S. Fasoulas, A. Mirza, P. Ortwein, M. Pfeiffer, T. Stindl, Coupled particle-in-cell and direct simulation Monte Carlo method for simulating reactive plasma flows, *C. R. Méc.* 342 (10) (2014) 660–670.
- [7] D.G. Shepherd, *Elements of Fluid Mechanics*, Harcourt, Brace and World, New York, 1965.
- [8] F. White, *Fluid Mechanics*, McGraw-Hill, New York, 2008.
- [9] J.H. Ernest Davidson, *Introduction to Plasma Technology*, Science, Engineering and Applications, WILEY-VCH Verlag and Co. KGaA, Singapore, 2010.
- [10] J.D. Huba, *NRL Plasma Formulary*, Naval Research Laboratory, Washington D. C., 2013.
- [11] R. Eckman, B. Lawrence, N.A. Gatsonis, E.J. Pencil, Triple Langmuir probe measurements in the plume of a pulsed plasma thruster, *J. Power Propul.* 17 (4) (2001) 762–771.
- [12] H. Goedbloed, S. Poedts, *Principles of Magnetohydrodynamics With Applications to Laboratory and Astrophysical Plasmas*, Cambridge University Press, Cambridge, 2004.
- [13] A. Dinklage, T. Klinger, G. Marx, L. Schweikhard, *Plasma Physics*, Springer, Berlin Heidelberg, 2008.
- [14] J.R. Roth, *Industrial Plasma Engineering*, Institute of Physics Publishing, Bristol, 1995.
- [15] U. Inan, M. Golkowski, *Principles of Plasma Physics for Engineers and Scientists*, Cambridge University Press, Cambridge, 2011.
- [16] A. Akkurt, The effect of cutting process on surface microstructure and hardness of pure and Al 6061 aluminium alloy, *Eng. Sci. Technol.* 18 (2015) 202–208.